RSC Advances

PAPER

View Article Online
View Journal | View Issue

Cite this: *RSC Adv.*, 2022, **12**, 772

Carboxylation of sodium arylsulfinates with CO_2 over mesoporous K-Cu-20TiO_2†

Yanjiao Chen, Xuan Dai, Wenwei Zhang, Tao Wu, Lei Chen and Xinhua Peng *

Received 7th July 2021
Accepted 5th November 2021

DOI: 10.1039/d1ra05228d

rsc.li/rsc-advances

A mesoporous ternary metal oxide (K-Cu-20TiO_2) from a simple sol–gel method was prepared to catalyze heterogeneously the carboxylation reaction of various sodium arylsulfinates under atmospheric carbon dioxide. The catalyst showed excellent selectivity and good functional group tolerance to carboxylation recycle. The oxidation state of active copper(I) by characterization using FTIR, XRD, TG, XPS and TEM techniques proved to be efficacious to conduct atom economical reactions.

1. Introduction

In recent years, the term "green chemistry" is frequently mentioned by researchers.[1] The emissions of carbon dioxide known as the "greenhouse gas" have far exceeded the level of pre-industry concentration.[2,3] Moreover, the utilization of CO_2 is rather attractive because of the abundant C1 source.[4–7] In spite of its high thermodynamic and kinetic stabilities, CO_2 has the characteristics of low electrophilicity.[8–10] Therefore, it is important to activate CO_2 with a Lewis acid to improve the electrophilic ability. For example, Olah *et al.* used the CO_2–Al_2Cl_6/Al system to carboxylate ethylbenzene in 33% yield of *p*-ethyl benzoic acid under 5.7 MPa CO_2 pressure.[11,12]

On the other hand, a strong carbon nucleophile acts on CO_2 to form valuable carboxylic acids and their derivatives.[13,14] The chemical utilization of CO_2 has made considerable progress.[15,16] In particular, some carbon nucleophiles such as Grignard reagents were employed to attack CO_2 in the syntheses of aliphatic carboxylic acids.[17,18] The reaction is usually conducted under strict anhydrous and anaerobic conditions.[19,20]

Some mild reaction conditions are developed towards the CO_2 carboxylation of organo-boron[21,22] and zinc substrates[23,24] in the presence of organometallic complexes. The reaction is accompanied by a cumbersome pre-functionalization process of the substrate and the requirements of sustainable chemistry are different.[25,26] Fujihara *et al.*[27–30] explored the carboxylation of aryl halides, styrene and propylene, *etc.* with CO_2 by synergy between reductants such as Mn or Zn and some organometallic complexes. These typical synthetic methodologies have been summarized in Scheme 1.

Various transition metal catalysts can catalyze the coupling reaction of sodium sulfonates involving Heck desulfurization reactions,[31] addition reactions of alkynes[32] and cross-coupling reactions with polyfluoroaromatic hydrocarbons.[33] Performing the carboxylation of sodium arylsulfinates with CO_2 (ref. 34) brings similar advantages, due to the stability and the processability of aromatic sodium sulfinates as aryl sources.[35,36]

In addition, it has been reported that the homogeneous catalyst CuI was used to catalyze the carbonylation reaction of CO_2 and sodium benzenesulfinate. However, CuI has the disadvantages of non-recoverability and easy loss of active sites. Recycling heterogeneous catalysts remains challenging. Here, the article describes a heterogeneous catalyst to promote the carboxylation of aromatic sodium arylsulfinates with CO_2.

The heterogeneous catalyst, a mesoporous ternary metal oxide (K-Cu-20TiO_2) is prepared using a sol–gel method by dissolving cheap polymers and metal alkoxides in a solution composed of glacial acetic acid, hydrochloric acid and ethanol (AcHE) (see ESI for details†).[37–40] K-Cu-20TiO_2 shows stable and

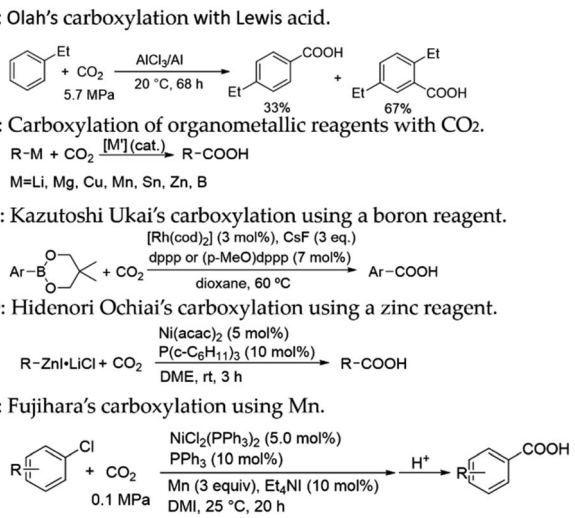

Scheme 1 The utilization of CO_2 in carboxylation reactions.

School of Chemistry and Chemical Engineering, Nanjing University of Science and Technology, Nanjing 210094, China. E-mail: xhpeng@njust.edu.cn; xinhpeng@njust.edu.cn

† Electronic supplementary information (ESI) available. See DOI: 10.1039/d1ra05228d

excellent catalytic performances and promotes the high-selective substitution carboxylation of arylsulfinates with CO_2 under mild conditions.

As shown in Fig. 1, 2 and 4, K-Cu-20TiO_2 from a uniform combination of potassium and copper components in *tetra*-butyl titanate stabilizes the oxidation state of active copper(I) based on the characterization of FTIR, XRD and XPS characterizations. In Fig. 3, the TG curve displays its good thermal stability up to 480 °C. In addition, it exhibits a high degree of uniformity with dense accumulation and mesoporous channels in the TEM image (Fig. 5).

2. Results and discussion

2.1. Characterizations of the catalyst

FTIR spectra of KNO_3, $Cu(NO_3)_2$, TiO_2 and K-Cu-20TiO_2 are depicted in Fig. 1. K-Cu-20TiO_2 exhibits the characteristic peaks of the stretching vibrations of KNO_3 at 2819–3006 cm^{-1} and 2360 cm^{-1} in Fig. 1(a). Similarly, the characteristic peak of TiO_2 stretching vibration at 3541–3868 cm^{-1} (Fig. 1(b)) exists in the spectrum of catalytic material, which shows the importance of the TiO_2 support.

XRD patterns of Cu-20TiO_2 and K-Cu-20TiO_2 are shown in Fig. 2. There is a strong 2θ peak at 25.3° corresponding to the (210) plane, which is attributed to TiO_2. The peaks at 36.2°, 48.0°, 54.3°, 54.5°, 62.0° and 68.9° are in good agreement with (102), (321), (230), (131), (502) and (040) planes of TiO_2 (PDF#72-0100), respectively. Peaks at 42.9° are consistent with the (221) plane of KNO_3 (PDF#81-0070).

The recorded TG curve of K-Cu-20TiO_2 is shown in Fig. 3. When 7.084 mg K-Cu-20TiO_2 is heated to 350 °C and 480 °C, the total mass loss is 0.275 and 0.492 mg, respectively. This shows that the catalyst demonstrates excellent thermal stability under reaction conditions.

XPS is used to characterize the Cu oxidation state. The existence of Cu(I) in fresh K-Cu-20TiO_2 is observed with the major peak at 929.9 eV (Fig. 4), which has no shake-up satellites in the range of 931–933 eV. It is demonstrated that Cu(I) ions are homogeneously incorporated into the TiO_2 matrix in mesoporous K-Cu-20TiO_2 materials.

TEM images in Fig. 5 are employed to analyze the morphology features of K-Cu-20TiO_2. From Fig. 5(a) to (e), the morphology of K-Cu-20TiO_2 is a tightly packed cubic structure with sizes in the range 2–50 nm, in which there are some pores on the surface of K-Cu-20TiO_2 as seen in Fig. 5(a). This proves

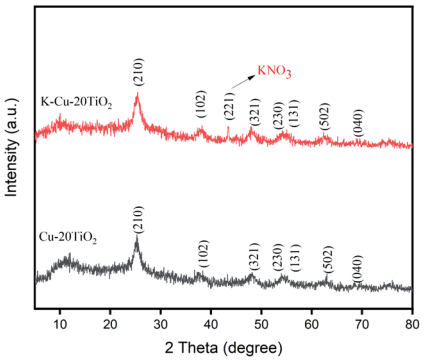

Fig. 2 XRD patterns of Cu-20TiO_2 and K-Cu-20TiO_2.

that TiO_2 is closely packed as a framework to form the mesoporous structure, while Cu and K are evenly dispersed and embedded in the crystal.

2.2. Optimization studies

The reaction of sodium benzenesulfinate with atmospheric CO_2 over the K-Cu-20TiO_2 catalyst turns out to be efficacious for the carboxylation with excellent selectivity. Control experiments were conducted with various bases, ligands and DMSO medium (Table 1). The reaction becomes rather weak in the absence of the catalyst as compared to that without the ligand or base (entries 1–3 in Table 1). Ligands and bases promote the reaction by synergy with the catalyst. Of the tested ligands, *o*-phenanthroline is the most effective as compared with other ligands such as pyridine, 2,2′-bipyridine, 4,4′-bipyridine and 2,2′,6′,2″-terpyridine in the presence of KO*t*Bu (entries 4–8 in Table 1). Of the tested bases, Cs_2CO_3 proves to be quite efficient when compared with its counterparts, such as K_2CO_3, KOH, $NaOC_2H_5$, LiO*t*Bu and KO*t*Bu, in the presence of *o*-phenanthroline (entries 4, 9–13 in Table 1). An optimum combination of the substrate (0.10 mmol), K-Cu-20TiO_2 (20.9 mg), *o*-phenanthroline (30 mol%) and Cs_2CO_3 (3.0 equiv.) in DMSO (2.5 mL) produced 85% conversion of sodium benzenesulfinate with 99.8% selectivity of benzoic acid during carboxylation (entry 10 in Table 1).

Moreover, the amounts of catalyst, ligand and base are able to affect the product yield (Table 2). The increase in the amount of the catalyst (entries 1–4 in Table 2), ligands (entries 5–7 in

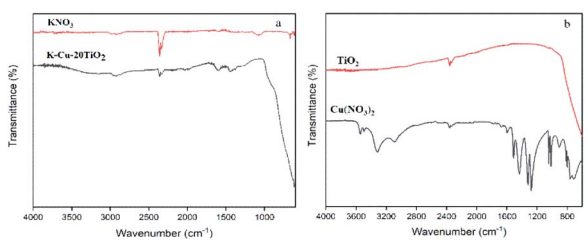

Fig. 1 FTIR spectra of (a) KNO_3 and K-Cu-20TiO_2, (b) TiO_2 and $Cu(NO_3)_2$.

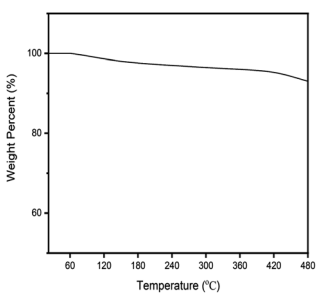

Fig. 3 TG curve of K-Cu-20TiO_2.

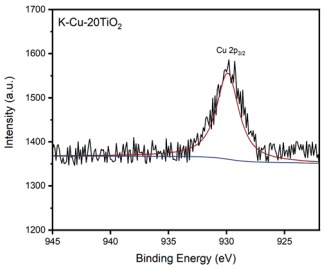

Fig. 4 XPS spectra of mesoporous K-Cu-20TiO_2.

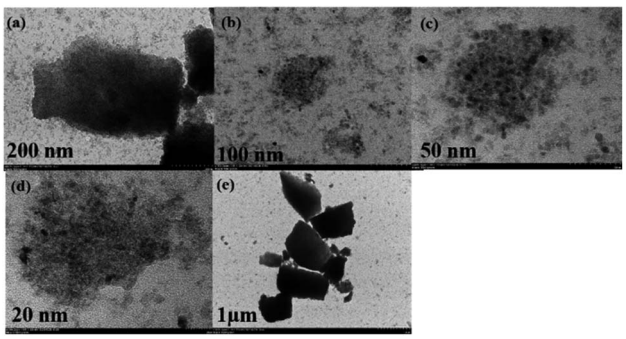

Fig. 5 TEM images of K-Cu-20TiO_2.

Table 1 Carboxylation of sodium benzenesulfinate with carbon dioxide[a]

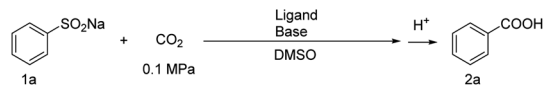

Entry	Catalyst	Ligand	Base	Conv.[b] (%)	Sel.[c] (%)
1	K-Cu-20TiO_2	—	KO*t*Bu	33	>99.2
2	K-Cu-20TiO_2	Phen	—	15	>99.3
3	—	Phen	KO*t*Bu	Trace	—
4	K-Cu-20TiO_2	Phen	KO*t*Bu	77	>99.5
5	K-Cu-20TiO_2	Py	KO*t*Bu	70	>99.5
6	K-Cu-20TiO_2	Bipy	KO*t*Bu	70	>99.4
7	K-Cu-20TiO_2	4,4′-Bipy	KO*t*Bu	60	>99.3
8	K-Cu-20TiO_2	Terpy	KO*t*Bu	50	>99.3
9	K-Cu-20TiO_2	Phen	K_2CO_3	80	>99.5
10	K-Cu-20TiO_2	Phen	Cs_2CO_3	85	>99.8
11	K-Cu-20TiO_2	Phen	KOH	73	>99.7
12	K-Cu-20TiO_2	Phen	$NaOC_2H_5$	55	>99.4
13	K-Cu-20TiO_2	Phen	LiO*t*Bu	50	>99.5

[a] The mixture of sodium benzenesulfinate (0.10 mmol), CO_2 (0.1 MPa), K-Cu-20TiO_2 (20.9 mg), ligand (0.03 mmol, phen: *o*-phenanthroline, py: pyridine, bipy: 2,2′-bipyridine, 4,4′-bipy: 4,4′-bipyridine, terpy: 2,2′,6′,2″-terpyridine, same as below), base (0.30 mmol) and DMSO (2.5 mL) was reacted at 120 °C for 16 h in a sealed Schlenk tube. [b] Conversion, determined by product yield and selectivity from GC and GC-MS analyses using 2-methylimidazole as internal standard. [c] Selectivity, mass percentage of benzoic acid in the product mixtures from GC and GC-MS analyses using 2-methylimidazole as internal standard.

Table 2 Screening the amount of catalyst, ligand and base[a]

Entry	K-Cu-20TiO_2 (mg)	Phen (mmol)	Cs_2CO_3 (mmol)	Conv.[b] (%)
1	62.9	0.03	0.30	87
2	41.8	0.03	0.30	86
3	20.9	0.03	0.30	85
4	10.5	0.03	0.30	41
5	20.9	0.04	0.30	86
6	20.9	0.02	0.30	75
7	20.9	0.01	0.30	35
8	20.9	0.03	0.40	87
9	20.9	0.03	0.20	72
10	20.9	0.03	0.10	55

[a] The mixture of sodium benzenesulfinate (0.10 mmol), CO_2 (0.1 MPa), K-Cu-20TiO_2, *o*-phenanthroline, Cs_2CO_3 and DMSO (2.5 mL) was reacted for 16 h at 120 °C in a sealed Schlenk tube. [b] Conversion, determined by product yield and selectivity from GC and GC-MS analyses using 2-methylimidazole as internal standard.

Table 2) and base (entries 8–10 in Table 2) can improve substrate conversion and carboxylation yield.

The carboxylation performance of various aromatic sodium arylsulfinates is inspected in optimum reaction conditions. As shown in Table 3, the reactions of arylsulfinates with CO_2 form corresponding carboxylated products smoothly with moderate substrate conversion and high product selectivity. These substrates with functional groups involving methyl, ethyl, methoxy, chloro, iodo and phenyl have no intimate relevance to the electron and conjugate effects by the electron-donating and electron-withdrawing groups on the aromatic ring.

The reusability of K-Cu-20TiO_2 for the carboxylation of sodium benzenesulfinate was investigated. The results under optimal conditions are shown in Fig. 6. It is clear that there are only insignificant decreases in conversion and selectivity after five cycles; the conversion and selectivity were about 83% and 99.8%, respectively. The catalyst is regenerated by the usual process involving centrifugation separation, washing with ethanol and deionized water, followed by drying at 70 °C prior to reuse.

The catalytic properties are implied by the mechanism presented in Scheme 2. Sodium benzenesulfinate in stronger alkaline conditions can favor metathesis from active Cu(I) of K-Cu-20TiO_2 based on the XPS analysis. The Cu(I) complex on solid surface is further coordinated with ligands to form an intermediate Ar–CuL (aromatic copper complex), accompanied by the release of molecular sulfur dioxide from the substrate. Subsequently, CO_2 is inserted into Ar–CuL to form a carbon–carbon coupling product of benzoate by the electrophilic substitution effect. This method based on the catalytic cycle can readily synthesize aromatic carboxylic acid by mild desulfination.

3. Experimental

3.1. Preparation and regeneration for catalyst

A mixture of 10 mmol $Ti(OBu)_4$, 40 mmol HOAc (99.5%), 12 mmol HCl (36–38%), 0.50 mmol $Cu(NO_3)_2 \cdot 3H_2O$ and 0.50 mmol KNO_3 was dissolved in 2 mL deionized water, and

Table 3 Extension of the substrate scope[a]

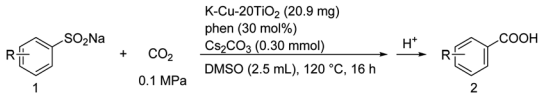

Entry	Substrate	Product	Conv.[b] (%)	Sel.[c] (%)
1	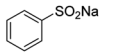	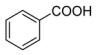	85	>99.8
2	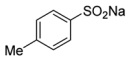	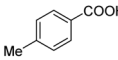	80	>99.6
3	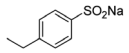	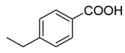	75	>99.3
4	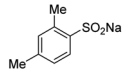	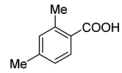	78	>99.6
5	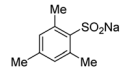	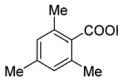	70	>99.3
6	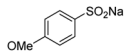	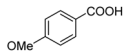	23	>99.1
7	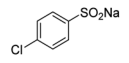	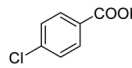	83	>99.3
8	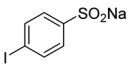	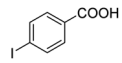	77	>99.3
9	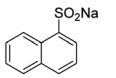	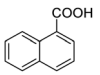	45	>99.4
10	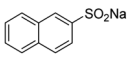	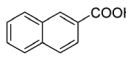	66	>99.5

[a] The mixture of substrate (0.10 mmol), CO_2 (0.1 MPa), K-Cu-20TiO_2 (20.9 mg), phen (0.03 mmol), Cs_2CO_3 (0.30 mmol) and DMSO (2.5 mL) was reacted for 16 h at 120 °C in a sealed Schlenk tube. [b] Conversion, determined by product yield and selectivity from GC and GC-MS analyses using 2-methylimidazole as internal standard. [c] Selectivity, mass percentage of benzoic acid in the product mixtures from GC and GC-MS analyses using 2-methylimidazole as internal standard.

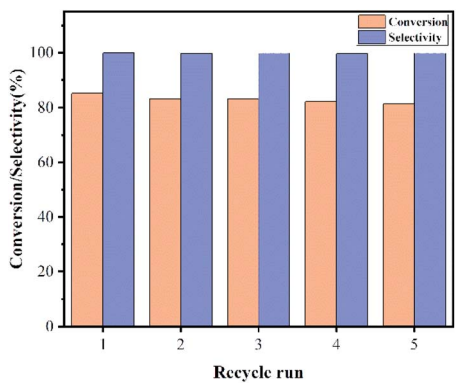

Fig. 6 Recycling of the catalyst.

1.6 g F68 (polyethylene-polypropylene glycol) in 30 mL ethanol was stirred vigorously for 1 h at room temperature. Then the mixture was further concentrated to form a yellow transparent film by rotary evaporation at 50 °C under reduced pressure. The film was aged for 24 h at 70 °C and then calcined for 5 h at 350 °C in nitrogen atmosphere. The film material was ground into a fine powder before use.

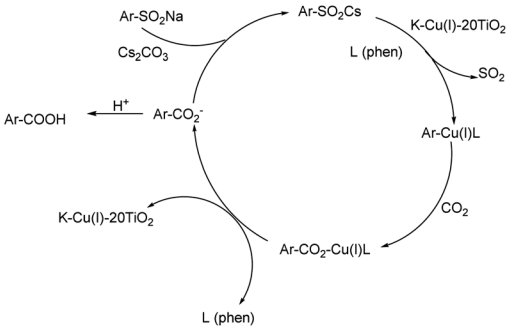

Scheme 2 The proposed electrophilic mechanism.

The solid catalyst separated from the reaction mixture by the centrifugation process was stirred for 1 h in 5.0 mL ethanol and then in 5.0 mL deionized water. After being aged for 24 h at 70 °C and then calcined for 5 h at 350 °C in nitrogen atmosphere, the solid was reused in the next run.

3.2. Procedure for carboxylation reaction

A 10 mL sealed Schlenk tube was ventilated with CO_2 added substrate (0.10 mmol), K-Cu-20TiO_2 (20.9 mg), ligand (0.03 mmol), base (0.30 mmol) and DMSO (2.5 mL). The mixture was stirred for 16 h at 120 °C under 0.1 MPa carbon dioxide atmosphere. After the mixture was cooled to room temperature, 1 mol L^{-1} HCl (1.5 mL) was added to the mixture. The catalyst was separated by centrifugation, and the product was extracted with EtOAc (5 mL × 3) and washed with saturated NaCl aqueous solution (5 mL × 3). The organic phase was dried by Na_2SO_4, and then concentrated by distillation and purified by TLC.

4. Conclusions

In summary, an excellent K-Cu-20TiO_2 catalyst is used to promote the atom economic carboxylation of CO_2 as the C1 source. Carboxylation of arylsulfinates does not need the usual pre-activation on the substrate in the presence of the solid catalyst. In addition, the reaction is heterogeneously performed in mild conditions on the solid surface with high product selectivity. Therefore, this methodology expands CO_2 fixation utilization.

Conflicts of interest

There are no conflicts to declare.

References

1 S. Fenner and L. Ackermann, *Green Chem.*, 2016, **18**, 3804–3807.

2 R. Zevenhoven, S. Eloneva and S. Teir, *Catal. Today*, 2006, **115**, 73–79.
3 S. N. Riduan and Y. Zhang, *Dalton Trans.*, 2010, **39**, 3347–3357.
4 T. Sakakura, J. C. Choi and H. Yasuda, *Chem. Rev.*, 2007, **107**, 2365–2387.
5 X. Gao, Z. Zhang, X. Wang, J. Tian, S. Xie, F. Zhou and J. Zhou, *Chem. Sci.*, 2020, **11**, 10414–10420.
6 A. Tortajada, F. Juliá-Hernández, M. Börjesson, T. Moragas and R. Martin, *Angew. Chem., Int. Ed.*, 2018, **130**, 16178–16214.
7 J. Louie, *Curr. Org. Chem.*, 2005, **9**, 605–623.
8 T. Ohishi, M. Nishiura and Z. Hou, *Angew. Chem., Int. Ed.*, 2008, **47**, 5792–5795.
9 J. Luo and I. Larrosa, *ChemSusChem*, 2017, **10**, 3317–3332.
10 M. Aresta, *Focus on Catalysts*, 2010, **4**, 1351–4180.
11 G. A. Olah, B. Torok, J. P. Joschek, I. Bucsi, P. M. Esteves, G. Rasul and G. K. Surya Prakash, *J. Am. Chem. Soc.*, 2002, **124**, 11379–11391.
12 Y. Suzuki, T. Hattori, T. Okuzawa and S. Miyano, *Chem. Lett.*, 2002, **31**, 102–103.
13 Q. Liu, L. Wu, R. Jackstell and M. Beller, *Nat. Commun.*, 2015, **6**, 5933.
14 T. E. Muller and W. Leitner, *Beilstein J. Org. Chem.*, 2015, **11**, 675–677.
15 Y. Kuwahara and H. Yamashita, *J. CO_2 Util.*, 2013, **1**, 50–59.
16 J. Rintjema, L. P. Carrodeguas, V. Laserna, S. Sopena and A. W. Kleij, *Top. Organomet. Chem.*, 2016, **53**, 39–71.
17 A. Correa and R. Martin, *Angew. Chem., Int. Ed.*, 2009, **48**, 6201–6204.
18 O. Vechorkin, N. Hirt and X. Hu, *Org. Lett.*, 2010, **12**, 3567–3569.
19 A. Nagaki, Y. Takahashi and J. Yoshida, *Chem.–Eur. J.*, 2014, **20**, 7931–7934.
20 A. Polyzos, M. O'Brien, T. P. Petersen, I. R. Baxendale and S. V. Ley, *Angew. Chem., Int. Ed.*, 2011, **123**, 1222–1225.
21 J. Takaya, S. Tadami, K. Ukai and N. Iwasawa, *Org. Lett.*, 2008, **10**, 2697–2700.
22 K. Ukai, M. Aoki, J. Takaya and N. Iwasawa, *J. Am. Chem. Soc.*, 2006, **128**, 8706–8707.
23 C. S. Yeung and V. M. Dong, *J. Am. Chem. Soc.*, 2008, **130**, 7826–7827.
24 H. Ochiai, M. Jang, K. Hirano, H. Yorimitsu and K. Oshima, *Org. Lett.*, 2008, **10**, 2681–2683.
25 K. Shimomaki, K. Murata, R. Martin and N. Iwasawa, *J. Am. Chem. Soc.*, 2017, **139**, 9467–9470.
26 X. Zhang, W. Z. Zhang, L. L. Shi, C. X. Guo, L. L. Zhang and X. B. Lu, *Chem. Commun.*, 2012, **48**, 6292–6294.
27 Y. Sato, M. Mori, M. Takimoto and M. Kawamura, *Synlett*, 2005, **134**, 2019–2022.
28 J. Takaya and N. Iwasawa, *J. Am. Chem. Soc.*, 2008, **130**, 15254–15255.
29 T. Fujihara, K. Nogi, T. Xu, J. Terao and Y. Tsuji, *J. Am. Chem. Soc.*, 2012, **134**, 9106–9109.
30 T. Moragas, M. Gaydou and R. Martin, *Angew. Chem., Int. Ed.*, 2016, **55**, 5053–5057.
31 G. W. Wang and T. Miao, *Chemistry*, 2011, **17**, 5787–5790.
32 S. Liu, Y. Bai, X. Cao, F. Xiao and G. Deng, *Chem. Commun.*, 2013, **49**, 7501–7503.
33 T. Miao and L. Wang, *Adv. Synth. Catal.*, 2014, **356**, 429–436.
34 S. Sun, J. Yu, Y. Jiang and J. Cheng, *Adv. Synth. Catal.*, 2015, **357**, 2022–2026.
35 W. Chen, P. Li, T. Miao, L. G. Meng and L. Wang, *Org. Biomol. Chem.*, 2013, **11**, 420–424.
36 M. Wang, D. Li, W. Zhou and L. Wang, *Tetrahedron*, 2012, **68**, 1926–1930.
37 J. Fan, S. W. Boettcher and G. D. Stucky, *Chem. Mater.*, 2006, **18**, 6391–6396.
38 P. Yang, D. Zhao, D. I. Margolese, B. F. Chmelka and G. D. Stucky, *Chem. Mater.*, 1999, **11**, 2813–2826.
39 D. Grosso, F. Cagnol, G. J. d. A. A. Soler-Illia, E. L. Crepaldi, H. Amenitsch, A. Brunet-Bruneau, A. Bourgeois and C. Sanchez, *Adv. Funct. Mater.*, 2004, **14**, 309–322.
40 J. Fan, Y. Dai, Y. Li, N. Zheng, J. Guo, X. Yan and G. D. Stucky, *J. Am. Chem. Soc.*, 2009, **131**, 15568–15569.